Maxwell-Wagner relaxations and their contributions to the high permittivity of calcium copper titanate ceramics

Wei Li and Robert W. Schwartz*
Department of Materials Science and Engineering, University of Missouri-Rolla, Rolla, Missouri 65409, USA
(Received 3 July 2006; revised manuscript received 9 August 2006; published 10 January 2007)

Calcium copper titanate ceramics were fabricated by cold isostatic pressing at various calcination and sintering conditions. Depending on fabrication condition, three electrical responses were observed in the combined modulus and impedance plots, indicating the presence of two Maxwell-Wagner relaxations. These electrical responses show different response to temperature and applied field. The activation energies, as well as the driving force factors, were calculated for these relations. The determined activation energy values are in the range of 0.57 to 0.65 eV. The contribution of Maxwell-Wagner relaxations to the high permittivity of CCTO and related materials is briefly discussed.

DOI: 10.1103/PhysRevB.75.012104 PACS number(s): 77.22.Ch, 77.22.Gm

Recently, $CaCu_3Ti_4O_{12}$ (CCTO) has attracted significant attention as a nonferroelectric material due to its high permittivity ($>10^5$) and weak temperature dependence of permittivity over a wide range (100–500 K). Although CCTO is typified by high loss, which has limited its utilization in practical applications, the origin of the high permittivity still warrants investigation. Since CCTO was first discovered,[1] a variety of models and experimental data on this material have been published. Researchers have gradually reached a consensus that Maxell-Wagner (M-W) polarization is the principal mechanism leading to the high permittivity exhibited by such materials.

M-W relaxation can be simulated by an equivalent circuit composed of two parallel constant phase elements (CPE) connected in series. Its frequency response spectrum is similar to that of Debye relaxation (dipole relaxation). M-W relaxation can occur for a variety of heterogeneities, including a depletion layer between a sample and electrode, and the interfacial layer of a grain boundary and/or domain boundary. Some reports[2–4] attributed the high permittivity to the presence of insulating grain boundaries with minimal electrode effects, although electrode effects do play an important role in some aspects.[5–8] Most recently, domain boundaries were suggested as another source at which M-W relaxation can occur.[4,9] It is important to discriminate the possible scenarios and their contributions to the high permittivity feature of CCTO.

In this paper, we report on combined Z'' and M'' studies of CCTO that have led to the identification of a third electrical response that is strongly influenced by the fabrication conditions. This response appears in addition to the electrical response of the grain and grain boundary regions. The possible origin and contribution of this response to permittivity is discussed based on its temperature and voltage dependencies.

CCTO powders were prepared by calcination of high purity $CaCO_3$, CuO, TiO_2 at 800, 850, 900, 950, and 1000 °C. Pellets were prepared by cold isostatic pressing at 300 MPa followed by sintering in air at 1040, 1060, 1080, 1100, and 1120 °C. Time at temperature was 12 h and the ramp rate employed was 5 °C/min. The crystal structure of the calcined powder and the final specimens were characterized by x-ray powder diffraction. All pellets were verified to be single phase CCTO. Impedance measurements were performed between 25 and 300 °C over the frequency range 1 Hz–1 MHz and dc bias range 0–9 V using a Solartron 1255B impedance analyzer at an oscillation voltage of 100 mV. Current-voltage measurements were carried out at room temperature using a Keithley electrometer (Model 236 Source Measurement Unit).

Figures 1(a)–1(e) shows the scanning electron microscopy (SEM) photomicrographs of CCTO powders calcined at 800, 850, 900, 950, and 1000 °C for 10 h, respectively. It is noted that the grain size increased with the increase of calcination temperature, finally reaching a value of approximately 1–2 μm at 1000 °C. Figure 1(f) illustrates the corresponding x-ray diffraction patterns. It was found that CCTO structure was formed even at 800 °C with the presence of TiO_2 and CuO peaks. The residual TiO_2 and CuO gradually disappeared with increasing calcination temperature.

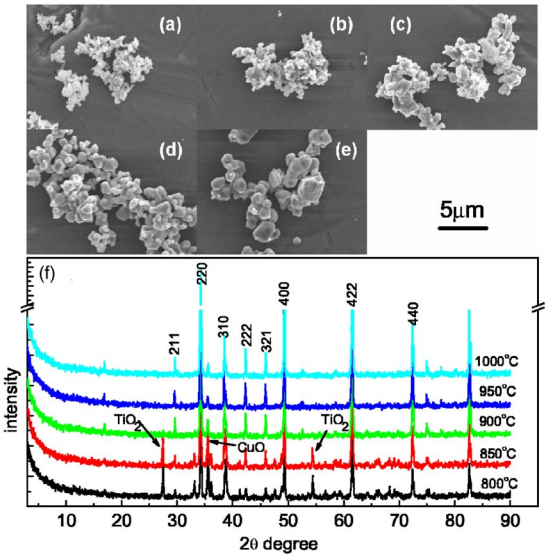

FIG. 1. (Color online) SEM photomicrographs of CCTO powders after calcination at 800 °C (a), 850 °C (b), 900 °C (c), 950 °C (d), and 1000 °C (e), respectively and their corresponding x-ray diffraction patterns (f).

TABLE I. Relative densities of CCTO for various calcination (C) and sintering (S) temperatures. Samples are divided into two classes: Class 1, and Class 2 (shown in bold text).

C/*S* Temp	1040 °C	1060 °C	1080 °C	1100 °C	1120 °C
800 °C	92.3%	92.6%	92.6%	92.6%	89.9%
850 °C	94.3%	94.0%	94.1%	92.3%	90.0%
900 °C	95.9%	97.1%	95.5%	93.4%	91.7%
950 °C	**97.6%**	**96.7%**	**95.9%**	93.2%	91.2%
1000 °C	**93.6%**	**93.4%**	**95.7%**	96.0%	91.7%

Table I shows the relative densities of CCTO specimens prepared at different calcination and sintering conditions as determined by the Archimedes method. The values are in the range of 89%–98%, which is greater than previously reported values.[2] The increased density is likely associated with the use of cold isostatic pressing. It was found that the distribution of the density values approximately obeys a commonly applied rule: with increasing temperature, density increases and then decreases above a threshold value. However, the increased density of CCTO specimens did not lower their dielectric loss due to the presence of M-W relaxation.

Combined Z'' and M'' plots are particularly useful to understand electrical behavior, since Z'' plots highlight phenomena characterized by the large resistance, whereas M'' plots identify electrical responses with small capacitance. The Z'' and M'' peaks for a particular resistor capacitor (RC) component should be coincident on the frequency scale[10] and a significant mismatch between Z'' and M'' peaks suggests localized conduction.[11] Figure 2 illustrates the combined Z'' and M'' plots for Class 1 and Class 2 specimens of Table I as a function of temperature and bias voltage. For visual consideration, all M'' data are divided by vacuum capacitance, C_0. Two (low and high frequency) and three (low, middle, and high frequency) electrical responses were observed in Class 1 and Class 2, respectively. For the low-frequency electrical response (LFER, $f<100$ Hz), both Z'' and M'' peaks shift to higher frequency with an increase of either temperature or dc bias voltage (M'' peaks for LFER of Class 2 are too small to be observed). This behavior indicates that the LFER is a thermally and electrically excited relaxation. For the high-frequency electrical response (HFER, $f>10^5$ Hz), the Z'' peaks are too small to be observed and only parts of the M'' peaks were found around 1 MHz with a much greater peak height. This result suggests that the HFER has a much lower resistance and capacitance. The LFER and HFER were attributed to the electrical response of the grain boundary and grain, respectively.[3,4] The increase in the M'' peak height of the LFER with voltage is in accordance with the fact that grain boundary capacitance decreases with applied dc bias.[12]

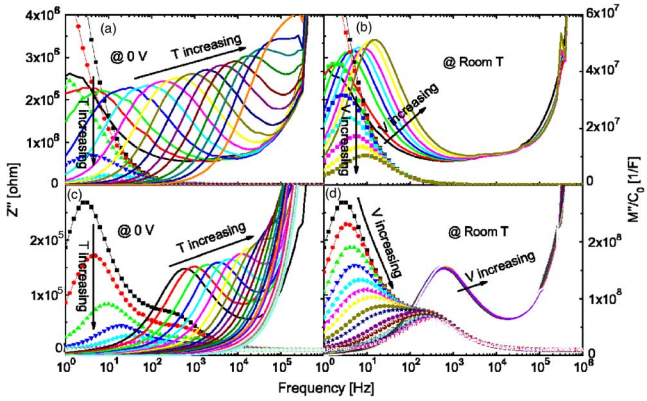

FIG. 2. (Color online) Combined Z'' and M'' plots of CCTO Class 1 and Class 2 specimens of Table I for various temperatures and bias voltages. Z'' plots are shown as symbol lines and M'' plots are shown as smooth lines. Arrows indicate the direction of increasing temperature and voltage. Temperature and voltage increase in sequence: (a) 25, 40, 60, 80, 100, 120, 140, 160, 180, 200, 220, 240, 260, 280, and 300 °C, (b) 0, 2, 4, 5, 6, 7, 8, and 9 V, (c) 25, 30, 40, 50, 60, 70, 80, 90, 100, 110, 120, 130, 140, 150, 160, 170, 200, 220, 240, 260, 280, and 300 °C, (d) 0, 0.1, 0.2, 0.3, 0.4, 0.5, 0.6, 0.8, 1, 1.5, 2, 3, 4, 5, 6, 7, 8, and 9 V.

The middle-frequency electrical response (MFER, $10^2<f<10^5$ Hz) can only be found in Class 2 materials, suggesting that this electrical response is dependent on fabrication conditions. Recent publications have addressed the occurrence of this response,[4,5] but its apparently different behavior compared with LFER has not been mentioned, i.e., its resistance and capacitance are independent of bias voltage, as seen in Fig. 2(d). Since LFER and MFER are thermally excited, an Arrhenius expression can be used to describe this process:

$$f_P = f_0 \exp(-E_a/k_B T), \tag{1}$$

where f_P is the peak frequency, f_0 is the preexponential factor, E_a is the activation energy, and k_B is the Boltzmann constant. A plot of $\ln(f_p)$ vs $1/T$, as shown in Fig. 3(a) yields the activation energies for the LFER of the Class 1, and the LFER, MFER of the Class 2 to be 0.65, 0.58, and 0.57 eV, respectively. These activation energies are very close to reported values of 0.60,[2] 0.68,[4] and 0.82 eV (Ref. 13) for the M-W relaxation associated with grain boundaries in CCTO.

The similar values of these activation energies strongly suggest that the associated relaxation processes originate from the same source, i.e., some kind of charge carriers such as electrons (or holes). The overlap of the Z'' and M'' peak positions in Fig. 2 indicates long-range conductivity. In oxides, the density n and activation energy U are two critical parameters to evaluate the long-range diffusion of charge carriers. The current density can be written as

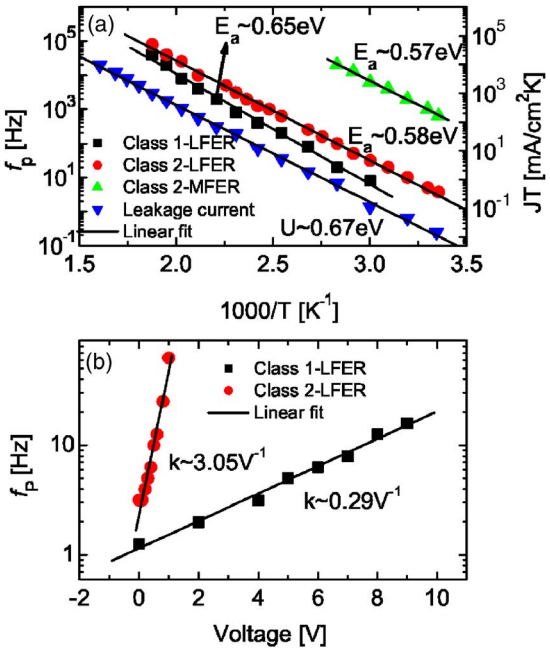

FIG. 3. (Color online) Peak frequency and leakage current density as a function of temperature (a) and peak frequency as a function of voltage (b).

$$J = \sigma_{dc}E = nq\mu E = \frac{nqD_0E}{T}\exp(-U/k_BT), \tag{2}$$

where q is the carrier charge, D_0 is the preexponential factor, and μ is the mobility of carriers. In order to avoid the abrupt increase in leakage current due to dielectric breakdown at high temperature, a small field of 30 V/cm was applied to the samples. The leakage current density as a function of temperature was measured and is plotted in Fig. 3(a). From the slope of the linear fit, the activation energy was calculated to be 0.67 eV, which lies within the range of expected values.

Since the LFER is also electrically excited, an equation similar to the Arrhenius law is proposed to describe this process

$$f_P = f_0\exp(kV), \tag{3}$$

where k is the driving force factor. As shown in Fig. 3(b), the collected data fall on straight lines. The driving force factors were determined to be 0.29 and 3.05 V^{-1} for the LFER of Class 1 and 2. The shift of the LFER peak frequency is due to the decrease of resistance and capacitance (the relaxation peak appears at $2\pi f_P RC=1$) with increase of the bias voltage and can be quantitatively defined using k as shown in Eq. (3). Values of k are related to the dielectric breakdown strength. The much larger k value of Class 2 indicates that the resistance and capacitance of the grain boundaries in Class 2 are more sensitive to the applied voltage than Class 1. Therefore, much lower dielectric breakdown strength will be in materials of Class 2. It is reasonable to believe that the different k values are due to the presence of the MFER in the Class 2 materials.

Next, the contribution of the three electrical responses to the high permittivity of CCTO should be discussed. In Class 1 materials, there are two electrical responses (grain and grain boundary). The imaginary parts of impedance and modulus can be expressed as

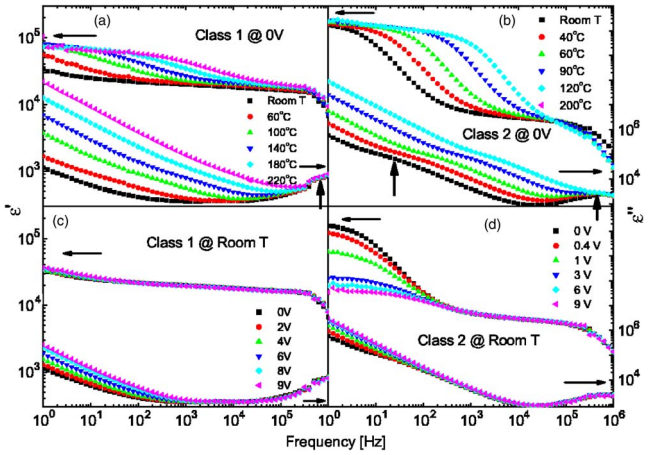

FIG. 4. (Color online) Real and imaginary parts of permittivity for Class 1 (a and b) and Class 2 (c and d) at various temperatures and bias voltages. The vertical arrows mark the positions where M-W relaxation occurs.

$$Z'' = R_1\left[\frac{\omega R_1C_1}{1+(\omega R_1C_1)^2}\right] + R_2\left[\frac{\omega R_2C_2}{1+(\omega R_2C_2)^2}\right]$$

and

$$M'' = \frac{C_0}{C_1}\left[\frac{\omega R_1C_1}{1+(\omega R_1C_1)^2}\right] + \frac{C_0}{C_2}\left[\frac{\omega R_2C_2}{1+(\omega R_2C_2)^2}\right]. \tag{4}$$

The permittivity will be

$$\varepsilon^* = \varepsilon' - i\varepsilon'' = \frac{1}{i\omega C_0Z^*} = \varepsilon'_\infty + \frac{\varepsilon'_s-\varepsilon'_\infty}{1+i\omega\tau} - i\frac{\sigma'}{\omega}, \tag{5}$$

where

$$\varepsilon'_\infty = 1/(C_0/C_1 + C_0/C_2),\ \varepsilon'_s = (R_1^2C_1 + R_2^2C_2)/C_0(R_1+R_2)^2,$$

$$\sigma' = \frac{1}{C_0(R_1+R_2)},\quad \text{and}\quad \tau = \frac{R_1R_2(C_1+C_2)}{(R_1+R_2)}.$$

In Z'' plot (or M'' plot), two peaks will appear at $1/2\pi R_1C_1$ and $1/2\pi R_2C_2$, respectively. Under zero bias and at room temperature, the peak frequency for the LFER is below 1 Hz while that for the HFER exceeds 1 MHz ($R_1 \gg R_2$ and $C_1 \gg C_2$). Therefore, only portions of the two peaks appear in Figs. 2(a) and 2(b). The shift of the peak frequency with temperature and voltage is due to a decrease in the resistance and capacitance. In the permittivity plot, ε'' peaks appear at $1/2\pi\tau=(R_1+R_2)/2\pi R_1R_2(C_1+C_2)\approx 1/2\pi R_2C_1$, and ε' demonstrates a relaxation (which appears as a step-function decrease). This frequency was calculated to be above 1 MHz, agreeing well with published results.[4]

Figure 4(a) and 4(b) show the permittivity of the Class 1 materials as a function of frequency for different temperatures and voltages. In the high frequency regime (>100 kHz), the ε'' curves begin to merge and form a peak

above 1 MHz, accompanying the steplike decrease in ε'. This Debye-like relaxation is the so-called M-W relaxation, which occurs at the interfacial layer between the grains and grain boundaries. The permittivity in the low and high frequency ranges is dominated by $\varepsilon_s' \approx C_{gb}/C_0$ (Ref. 3) and $\varepsilon_\infty' \approx C_g/C_0$, respectively. However, in the Class 2 materials, there are three electrical responses: LFER $(1/2\pi R_1 C_1)$, HFER $(1/2\pi R_2 C_2)$, and MFER $(1/2\pi R_3 C_3)$. By equivalent circuit simulation, the RC elements were determined to be $R_1=803$ kΩ, $C_1=71.2$ nF for the LFER, and $R_3=97.5$ kΩ, $C_3=3.61$ nF for the MFER. The RC elements for the HFER were not analyzed in this work because they have been explored in great detail previously. They are significantly smaller than those of the LFER and MFER. Figures 4(c) and 4(d) shows the permittivity of the Class 2 materials as a function of frequency at various temperatures and voltages. As mentioned for the Class 1 material, the M-W polarization associated with interfacial layers appears above 1 MHz. There is another M-W polarization in the middle-frequency range. The ε'' peak frequency was calculated to be $1/2\pi\tau = (R_1+R_3)/2\pi R_1 R_3 (C_1+C_3) = 24.5$ Hz. The anomalies of ε'' curves at this frequency in Figs. 4(c) and 4(d) demonstrate the presence of the second M-W polarization, accompanied by an obvious step decrease of ε'. Further calculation indicates that $\varepsilon_s' = 153132$ and $\varepsilon_\infty' = 9286$. The decrease of ε_s' in low-frequency range with voltage shown in Fig. 4(d) is due to the decrease of grain boundary resistance (i.e., LFER; the resistance of the MFER remains constant) [Fig. 2(d)]. Therefore, it may be concluded that the permittivity of CCTO is dominated by grain boundary behavior in low-frequency range ($f < 100$ Hz), by the grain phase in high-frequency range ($f > 10^5$ Hz), and by other structural or material characteristics (that are associated with the MFER) in middle-frequency range ($100 < f < 10^5$ Hz).

The final challenge is to determine the material characteristics associated with the relaxation phenomena that lead to the MFER. Unfortunately, little information has been reported in this area. Domain boundaries and depletion layers represent two possible choices. The capacitance of a depletion layer is strongly influenced by applied voltages through

$$C = \sqrt{e\varepsilon' N d/2(V_d + V)}, \tag{6}$$

where V_d is the diffusion potential and N_d is the concentration of donors.[7] Because the capacitance for the MFER shown in Fig. 2(d) did not display this tendency, it seems unlikely that depletion layers are the origin of the MFER. Domain boundaries represent insulating barriers in CCTO ceramics and their presence has been confirmed by transmission electron microscopy and small area electron diffraction (SAED).[14] The effective capacitance of a domain boundary is determined by the ratio of the domain boundary area to the grain size, consistent with the fact that CCTO single crystals exhibit large dielectric constants when twin boundaries, or planar dislocations, are present.[15] The location of Class 2 CCTO materials in Table I (lower left) can be explained by the competition between grain size and microstructural quality (e.g., porosity development, grain integrity, and defect density). As sintering temperature is initially increased, grain size increases, favoring the development of domain boundaries. With further increases in sintering temperature, microstructural quality is degraded, resulting in a decrease in the number of domain boundaries with a corresponding minimization of the MFER.[4,9,14,16] However, domain boundaries are considered to possess larger resistance and capacitance than grain boundaries, due to their lower thickness and larger area per unit volume.[4] Whether domain boundaries are the dielectric origin of the MFER and why the associated capacitance did not vary with applied voltage still warrant further investigation.

This work was supported by a MURI Program sponsored by the Office of Naval Research under Grant. No. N000-14-05-1-0541.

*Corresponding author. Email address: rwschwar@umr.edu

[1] M. A. Subramanian, D. Li, N. Duan, B. A. Reisner, and A. W. Sleight, J. Solid State Chem. **151**, 323 (2000).
[2] D. C. Sinclair, T. B. Adams, F. D. Morrison, and A. R. West, Appl. Phys. Lett. **80**, 2153 (2002).
[3] J. Liu, C. Duan, W. Mei, R. Smith, and J. Hardy, J. Appl. Phys. **98**, 093703 (2005).
[4] J. L. Zhang, P. Zheng, C. L. Wang, M. L. Zhao, J. C. Li, and J. F. Wang, Appl. Phys. Lett. **87**, 142901 (2005); S. F. Shao, J. L. Zhang, P. Zhang, W. L. Zhong, and C. L. Wang, J. Appl. Phys. **99**, 084106 (2006).
[5] P. Lunkenheimer, R. Fichtl, S. G. Ebbinghaus, and A. Loidl, Phys. Rev. B **70**, 172102 (2004); B. Renner, P. Lunkenheimer, M. Schetter, A. Loidl, A. Reller, and S. G. Ebbinghaus, J. Appl. Phys. **96**, 4400 (2004).
[6] C. Verdier, F. D. Morrison, D. C. Lupascu, and J. F. Scott, J. Appl. Phys. **97**, 024107 (2005).
[7] J. Yu, T. Ishikawa, Y. Arai, S. Yoda, M. Itoh, and Y. Saita, Appl. Phys. Lett. **87**, 252904 (2005).
[8] C. C. Wang and L. W. Zhang, Appl. Phys. Lett. **88**, 042906 (2006).
[9] T. T. Fang and H. K. Shiau, J. Am. Ceram. Soc. **87**, 2072 (2004).
[10] D. C. Sinclair and A. R. West, J. Appl. Phys. **66**, 3850 (1989).
[11] M. A. L. Nobre and S. Lanfredi, J. Appl. Phys. **93**, 5576 (2003).
[12] T. B. Adams, D. C. Sinclair, and A. R. West, Phys. Rev. B **73**, 094124 (2006).
[13] I. Kim, A. Rothschild, and H. Tuller, Appl. Phys. Lett. **88**, 072902 (2006).
[14] S. Y. Chung, I. D. Kim, and S. J. L. Kang, Nat. Mater. **3**, 774 (2004); S. Y. Chung, Appl. Phys. Lett. **87**, 052901 (2005).
[15] C. C. Homes, T. Vogt, S. M. Shapiro, S. Wakimoto, and A. P. Ramirez, Science **293**, 673 (2001).
[16] B. A. Bender and M.-J. Pan, Mater. Sci. Eng., B **117**, 339 (2005).